Accepted Manuscript

Furanoflavones Pongapin and Lanceolatin B Blocks the Cell Cycle and Induce Senescence in CYP1A1-overexpressing Breast Cancer Cells

Rajni Sharma, Ibidapo S. Williams, Linda Gatchie, Vinay R. Sonawane, Bhabatosh Chaudhuri, Sandip B. Bharate
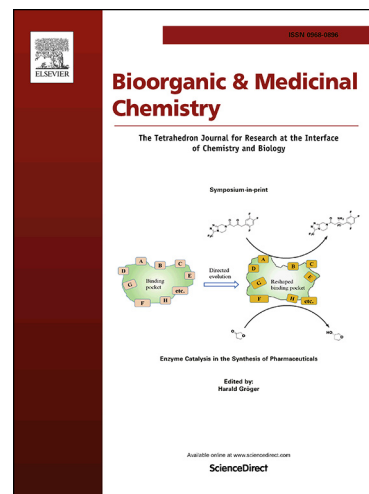
Please cite this article as: Sharma, R., Williams, I.S., Gatchie, L., Sonawane, V.R., Chaudhuri, B., Bharate, S.B., Furanoflavones Pongapin and Lanceolatin B Blocks the Cell Cycle and Induce Senescence in CYP1A1-overexpressing Breast Cancer Cells, *Bioorganic & Medicinal Chemistry* (2018), doi: https://doi.org/10.1016/j.bmc.2018.11.013

Furanoflavones Pongapin and Lanceolatin B Blocks the Cell Cycle and Induce Senescence in CYP1A1-overexpressing Breast Cancer Cells

Rajni Sharma,[a#] Ibidapo S. Williams,[b#] Linda Gatchie,[b] Vinay R. Sonawane,[b] Bhabatosh Chaudhuri,[b,c]* Sandip B. Bharate*[a]

[a] *CSIR-Indian Institute of Integrative Medicine, Canal Road, Jammu-180001, India.*

[b] *CYP Design Ltd, The Innovation Centre, 49 Oxford Street, Leicester LE1 5XY, UK*

[c] *Leicester School of Pharmacy, De Montfort University, Leicester, LE1 9BH, UK.*

*Corresponding authors

* Tel: +91 191 2569006; Fax: +91 191 2569333; E-mail: sbharate@iiim.ac.in (SBB).

*Tel: 00-44-7805230121; E-mail: bchaud00@gmail.com (BC)

[#]*RS and ISW contributed equally as a first author.*

ABSTRACT

Expression of cytochrome P450-1A1 (CYP1A1) is suppressed under physiologic conditions but is induced (a) by polycyclic aromatic hydrocarbons (PAHs)which can be metabolized by CYP1A1 to carcinogens, and (b) in majority of breast cancers. Hence, phytochemicals or dietary flavonoids, if identified as CYP1A1 inhibitors, may help in preventing PAH-mediated carcinogenesis and breast cancer. Herein, we have investigated the cancer chemopreventive potential of a flavonoid-rich Indian medicinal plant, *Pongamia pinnata* (L.) Pierre. Methanolic extract of its seeds inhibits CYP1A1 in CYP1A1-overexpressing normal human HEK293 cells, with IC_{50} of 0.6 µg/mL. Its secondary metabolites, the furanoflavonoids pongapin/ lanceolatin B, inhibit CYP1A1 with IC_{50} of 20 nM. Although the furanochalcone pongamol inhibits CYP1A1 with IC_{50} of only 4.4 µM, a semisynthetic pyrazole-derivative **P5b**, has ~10-fold improved potency (IC_{50}, 0.49 µM). Pongapin/ lanceolatin B and the methanolic extract of *P. pinnata* seeds protect CYP1A1-overexpressing HEK293 cells from B[a]P-mediated toxicity. Remarkably, they also block the cell cycle of CYP1A1-overexpressing MCF-7 breast cancer cells, at the G_0-G_1 phase, repress cyclin D1 levels and induce cellular-senescence. Molecular modeling studies demonstrate the interaction pattern of pongapin/lanceolatin B with CYP1A1. The results strongly indicate the potential of methanolic seed-extract and pongapin/lanceolatin B for further development as cancer chemopreventive agents.

KEYWORDS: Furanoflavones; Pongapin; Lanceolatin B; Cell Cycle; Senescence; CYP1A1

1. INTRODUCTION

The polycyclic aromatic hydrocarbons (PAHs) belong to a ubiquitous group of environmental procarcinogens, which have two or more fused aromatic (benzene) rings. The PAHs are generated primarily from coal tar, tobacco smoke, wood burning and grilled meats.[1] The low-molecular-weight PAHs (which contain 2-3 rings) occur in the atmosphere predominantly in the vapor phase, whereas multi-ringed PAHs (which contain 5 rings or more) are largely bound to environment-borne fine particles. In particular, the particle-bound PAHs are considered to be highly hazardous to human health. One of the most common particle-bound PAH is benzo[a]pyrene (B[a]P). Concentrations of B[a]P in human plasma is often used as a marker for exposure to carcinogenic PAHs, as the contribution of B[a]P to the total carcinogenic potential has been reported to be very high.[2] On human exposure, B[a]P undergoes metabolic activation by cytochrome P450-1A1 (CYP1A1) enzyme which is an extrahepatic phase I metabolizing enzyme that is suppressed under physiologic conditions. CYP1A1 is induced, via the aromatic hydrocarbon receptor (AhR), by PAHs which act as ligands of AhR.[3-6] The procarcinogen B[a]P, which also induces CYP1A1 expression via AhR, is metabolized by CYP1A1 to carcinogenic benzo[a]pyren-7,8-dihydrodiol-9,10-epoxide[7, 8] which is mutagenic, highly carcinogenic and is listed as a group 1 carcinogen by the International Agency for Research on Cancer (IARC).[7, 9] The role of human CYP enzymes in procarcinogen metabolism has been studied extensively[10] and it is the CYP1A1 enzyme that primarily plays a major part in B[a]P activation.[7, 10, 11] Therefore, inhibitors of CYP1A1 have extensively been investigated with the goal of discovering chemical agents that would prevent cancer[12, 13] by overcoming PAH-mediated carcinogenicity.[14-21]

Although CYP1A1 is practically non-existent in normal breast tissues, its levels are relatively high, depending on the grade of the tumor, in majority of breast cancer tumors.[22, 23] Because of CYP1A1's pervasive expression in breast cancer; there is interest in modulating CYP1A1 activity for breast cancer therapeutics.[24-27] Small interfering RNA (siRNA) molecules have been used to investigate the consequence of knocking down CYP1A1 mRNA levels. It was seen that CYP1A1-expressing breast cancer cells arrest at G_0-G_1 phase of the cell cycle and are associated with reduction of cyclin D1 and increased apoptosis.[28] Interestingly, inhibition of proliferation was not at all affected by α-naphthoflavone (ANF).[29] Although ANF is a known CYP1A1 microsomal enzyme inhibitor, it is highly insoluble and does not inhibit CYP1A1 enzyme within live cells.[19, 21, 30]

Pongamia pinnata (L.) Pierre (Family: Fabaceae) is an Indian beech tree which has been reported to possess many medicinal properties.[31-44] Pongamol, the major constituent of this plant, is also reported as an antiproliferative[45] and an antihyperglycemic agent.[46] Since karanjin and pongamol, the chemical constituents of *Pongamia pinnata*, induce NQO1 [NAD(P)H quinine oxidoreductase 1] they have been reported as cancer chemopreventive agents [47]. Recently we reported karanjin as a potent CYP1 inhibitor which could act to protect cells from undergoing carcinogenesis.[48] However, the CYP1A1 inhibitory potential of *P. pinnata* (L.) Pierre extracts or its other constituents have never been explored. The seeds of this tree are reported to contain many flavonoids. Therefore, the present study was primarily aimed to investigate the potential of *Pongamia pinnata* seed extracts and its chemical constituents to inhibit CYP1A1 using (a) Sacchrosomes™ (i.e. microsomal enzymes which areisolated from whole yeast cells) and (b) live normal human kidney cells HEK293, grown in suspension, which overexpress CYP1A1 protein.[20, 48, 49] The selectivity of the potent CYP1A1 inhibitors, over other CYP1, CYP2 and

4

CYP3 sub-family of enzymes, was determined. The most potent inhibitors isolated from *P. pinnata*, of CYP1A1 (i.e. the furanoflavones[50] pongapin and lanceolatin B) and the methanolic seed extract of *P. pinnata* were further studied to see if they would overcome B[a]P mediated toxicity in CYP1A1-overexpressing normal human HEK293 cells.[20, 48, 49] Furthermore, pongapin and lanceolatin B were used to examine if they would inhibit recombinant human breast cancer MCF-7 cells that overexpress CYP1A1 (referred to as MCF7-1A1 cells).

2. RESULTS AND DISCUSSION

2.1. Furanoflavones from *Pongamia pinnata* Potently Inhibit CYP1A1 and CYP1B1. The methanolic extract (ME) of *Pongamia pinnata* seeds showed potent inhibition of CYP1A1 and CYP1B1 in Sacchrosomes™ as well as in live HEK293-CYP1A1 cellular assay. The IC_{50} values for inhibition of CYP1A1 and CYP1B1 in live cells were 0.6 and 0.4 μg/mL, respectively (Table S1, supporting information). The interesting CYP1 (i.e. CYP1A1 and CYP1B1) inhibitory activity of extracts indicated that further phytochemical investigation of methanolic extract may provide an opportunity to discover new potent CYP1 inhibitors.

The ME was partitioned with different organic solvents *viz*. hexane, ethyl acetate, chloroform and *n*-butanol. Repeated column chromatography of ethyl acetate fraction led to the isolation of five compounds, which were characterized by comparison of their spectral data with literature values. The isolated compounds include karanjin, pongamol, pongapin, ovalitenone, and pongol. The two furanoflavoneslanceolatin B and pongaglabrone which naturally occur in seeds of this tree, were synthesized from furano-hydroxychalcones pongamol and ovalitenone by treatment with potassium carbonate in DMF.[51]

All isolated natural products karanjin, pongol, pongapin, pongamol and ovalitenone along with synthesized natural products lanceolatin B and pongaglabrone were first tested for inhibition of CYP1A1 and CYP1B1 in Sacchrosomes™, baker's yeast derived isolated microsomal enzymes (Table 1). Amongst the 7 compounds, pongapin, ovalitenone, pongol, and lanceolatin B displayed potent inhibition of CYP1A1 with IC_{50} values in the range of 71-690 nM. The most potent CYP1A1 inhibitors were the furanoflavones, pongapin and lanceolatin B, showing IC_{50} values of 71 and 76 nM, respectively. Next, all the 7 compounds were tested for inhibition of CYP1A1 and CYP1B1 enzymes expressed within live HEK293 cells. Karanjin displayed potent inhibition of CYP1A1 as well as CYP1B1,expressed within HEK293 cells, with IC_{50} values of 0.03 and 0.22 μM, respectively.[48] Furanoflavones, pongapin and lanceolatin B, displayed potent inhibition of CYP1A1, with the same IC_{50} value of 20 nM in the live HEK293 cellular assay. As CYP1A1 inhibitors, pongapin and lanceolatin B had 53 and 19.5-fold specificity vis-à-vis the CYP1B1 enzyme in live HEK293 cells, that individually expressed the two enzymes (Table 1). We have found that the true potential of a chemical compound or a natural product to inhibit a CYP enzyme can be determined ideally using CYP enzyme activities expressed within live human HEK293 cells rather than with CYP enzymes bound to endoplasmic reticular membranes which are isolated from recombinant cells, and which are referred to as microsomal enzymes (commercially available as Sacchrosomes™, Baculosomes™, Bactsosomes™ or Supersomes™). Our findings areanalogous to the fact that human hepatocytes are generally preferred to microsomal enzymes by the pharmaceutical industry for IC_{50} and drug metabolism studies and would have widely been used if they were more readily available for routine use.[52] Using US Food and Drug Administration (FDA)-approved CYP inhibitors, we have seen that IC_{50} values for inhibition of CYPs expressed in HEK293 cells are very similar to that obtained using human

hepatocytes, and often have stark differences to IC_{50} values obtained using microsomal enzymes (manuscript in preparation).
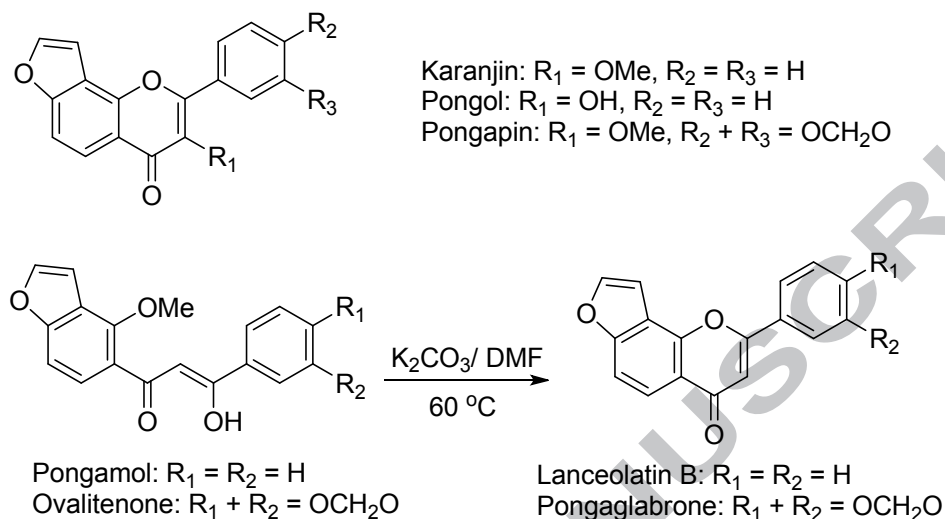

Figure 1. The structures of *Pongamia pinnata* constituents isolated or semi-synthetically prepared. Karanjin, pongol, pongapin, pongamol and ovalitenone were isolated from *Pongamia pinnata*. Lanceolatin and pongaglabrone were synthesized from pongamol and ovalitenone, respectively.

Table 1. In vitro CYP1A1 and CYP1B1 inhibitory activity of isolated constituents of *P. pinnata* in live human HEK293 cells, grown in suspension, that bear the human *CYP1A1*/*CYP1B1* genes and which overexpress the CYP1A1/CYP1B1enzymes. [a]

Entry	IC_{50} (µM) ± SD (Sacchrosomes™)		IC_{50} (µM) ± SD (HEK293)	
	CYP1A1	CYP1B1	CYP1A1	CYP1B1
Karanjin	2.7 ± 0.5	4.1 ± 0.6	0.03 ± 0.008	0.03 ± 0.008
Pongamol	2.4 ± 0.5	3.9 ± 0.7	4.4 ± 0.9	4.5 ± 0.8
Pongapin	0.071 ± 0.008	0.95 ± 0.12	0.02 ± 0.005	1.06 ± 0.06

7

Ovalitenone	0.28 ± 0.07	0.6 ± 0.5	0.48 ± 0.15	1.5 ± 0.6
Pongol	0.69 ± 0.11	3.8 ± 0.8	0.24 ± 0.11	1.2 ± 0.2
Lanceolatin B	0.076 ± 0.008	0.29 ± 0.07	0.02 ± 0.005	0.39 ± 0.12
Pongaglabrone	8.2 ± 1.2	3.4 ± 0.7	6.4 ± 0.9	6.8 ± 1.1
ANF[b]	0.05 ± 0.02	0.04 ± 0.02	>10	>10

[a]All values represent mean and standard deviations (± SD) from three independent experiments. [b] ANF (alpha-naphthoflavone) is a positive control used in this experiment.

2.2. Semisynthetic Modification of the Furanochalcone, Pongamol, a Major Constituent of *Pongamia pinnata*, Results in Improved CYP1A1 inhibition.

Pongamol is the major bioactive constituent of this plant;[53] therefore, it was isolated in gram quantities. Chemically, pongamol has a keto-enol functionality which provides an interesting handle for synthetic modifications. As described earlier, by base-mediated ring cyclization we could convert pongamol to the furanoflavone, lanceolatin B.[51] Further, we were interested in cyclizing this keto-enol functionality in the form of a heterocycle. Pongamol exists in keto-enol tautomeric forms (β-keto dihydrochalcone and β-hydroxychalcone).[54] Treatment of pongamol with hydroxylamine hydrochloride, in the presence of acetic acid, resulted in formation of oxazole derivatives **P1a** and **P1b** in combined yields of 60%. Pair of regioisomers were formed in each reaction because of the presence of pongamol in two states, as β-keto dihydrochalcone and as β-hydroxychalcone. When pongamol was treated with different substituted phenyl hydrazines, a series of regioisomeric pairs of pyrazole derivatives **P2a-P7a** and **P2b-P7b** were obtained in 52-73% yield (Figure 2A). All pairs of regioisomers were separated from each other, using semi-preparative HPLC. All compounds were characterized by NMR and MS analysis.

8

The ^{1}H NMR spectrum of the mixture of a representative regioisomeric pair **P7a** and **P7b** clearly showed the presence of two singlets at δ 3.70 and 4.11 ppm, indicating the presence of two methoxy groups, one each for a regioisomer. Similarly, the ^{13}C NMR spectrum showed two distinct peaks at δ 59.8 (OMe) and 60.5 ppm (OMe). It is interesting to mention that the pair of regioisomers showed a uniform pattern of HPLC retention times and chemical shift values for OMe groups in the pair of isomers. Thus, these findings can be generalized for this class of compounds. The HPLC retention times and OMe signals in the NMR spectra of these pairs of regioisomers are summarized in Figure 2B. In all cases, one particular isomer is eluted faster than the other from the HPLC column. Similarly, the methoxy signal of 2′-phenyl isomers is downfield shifted in both ^{1}H and ^{13}C NMR in comparison to the methoxy signal of 1′-phenyl isomers. The final confirmation and assignment of the regioisomers was done by recording single crystal X- ray crystal structure of one representative pair **P7a/P7b**. The ORTEP (Oak Ridge Thermal Ellipsoid Plot Program) diagrams of these isomers are shown in Figure 2C.
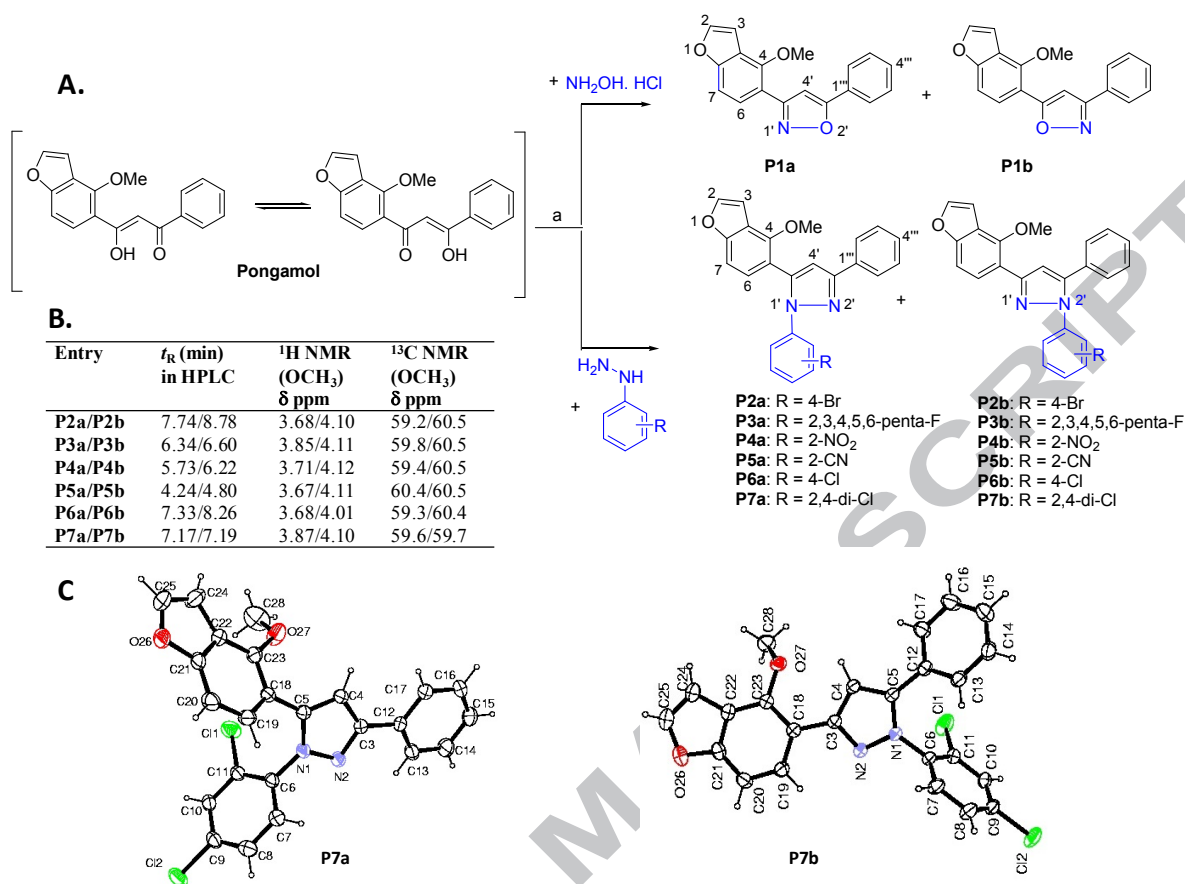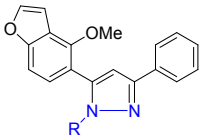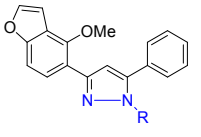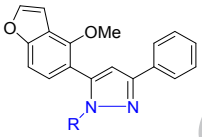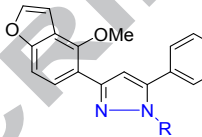
Figure 2. (A). Synthesis of pongamol derivatives **P1a-P7a, P1b-P7b**. Reagents and conditions: (a) CH₃COOH, 70 °C, 4 h, 52-73%. (B). Parameters (HPLC retention time and NMR chemical shift values) to distinguish a pair of regioisomers. (C) ORTEP diagram of regioisomer **P7a** and **P7b**.

All synthesized derivatives were tested for inhibition of CYP1A1/ CYP1B1 in Sacchrosomes™ at 10 μM concentration. Among all the derivatives tested, the compounds **P4b**, **P5a** and **P5b** showed promising inhibition (>70%) of CYP1A1 in Sacchrosomes™. However, none of the compounds was much effective against CYP1B1. Furthermore, out of the two positional isomers, particularly the one isomer e.g. **P4a** *versus* **P4b** – the isomer 'b' is more active than 'a'. A similar trend was observed among all pairs (Table 2). The compounds **P4b**, **P5a** and **P5b** also showed potent inhibition of CYP1A1 in live recombinant human HEK293 cells (>84% inhibition at 10 µM).

10

Table 2. In vitro CYP1A1 and CYP1B1 inhibitory activity of pongamol derivatives in Sacchrosomes™ (yeast derived microsomal enzymes), at 10 μM concentration.

	% inhibition at 10 μM (Sacchrosomes™)[a]			
Regio-isomeric pair	**CYP1A1**		**CYP1B1**	
	P2a-P7a	**P2b-P7b**	**P2a-P7a**	**P2b-P7b**
P1a/P1b[b]	36.1 ± 2.4	48.9 ± 1.6	2.3 ± 2.2	0.6 ± 0.1
P2a/P2b	27.9 ± 4.2	49.5 ± 3.2	1.1 ± 0.6	20.7 ± 0.9
P3a/P3b	30.6 ± 1.5	68.3 ± 2.7	0.7 ± 0.3	0 ± 0.03
P4a/P4b	31.6 ± 1.9	88.8 ± 2.4	3.9 ± 2.8	46 ± 1.5
P5a/P5b	85.7 ± 4.2	95.4 ± 3.5	67.8 ± 2.2	28.1 ± 2.3
P6a/P6b	9.7 ± 0.3	47.4 ± 2.8	2.3 ± 0.3	16.8 ± 1.2
P7a/P7b	28.6 ± 4.3	53.7 ± 5.1	2.2 ± 1.2	3.3 ± 0.6
ANF[c]	97 ± 3.5		98 ± 2.2	

[a]All values represent mean and standard deviations (± SD) from three independent experiments. [b] the regioisomeric pair **P1a/ P1b** contains "3-(4-methoxybenzofuran-5-yl)-5-phenylisoxazole" as **P1a** whereas "5-(4-methoxybenzofuran-5-yl)-3-phenylisoxazole" as **P1b**. The structures of this pair are shown in Figure 2. [c]ANF (alpha-naphthoflavone) is a positive control used in this experiment.

Next, for determination of IC_{50} for inhibition of CYP1A1 and CYP1B1 enzymes, the best pair **P5a**/ **P5b**, was chosen as a representative example (Table 3). The isomers **P5a** and **P5b** inhibited CYP1A1 enzyme in live HEK293 cell assays, with IC_{50} values of 8.6 and 0.49 µM, respectively. The results indicate that the derivative **P5b** possesses 10-fold higher CYP1A1 inhibitory activity than its parent natural product pongamol (IC_{50}, 4.4 µM).

Table 3. IC_{50} values for inhibition of CYP1A1 and CYP1B1 for selected regioisomeric pairsusing Sacchrosomes™ and CYP-expressing live HEK293 cells.

Entry	IC_{50} (µM) ± SD (Sacchrosomes™)[a]		IC_{50} (µM) ± SD (HEK293)[a]	
	CYP1A1	CYP1B1	CYP1A1	CYP1B1
Pongamol	2.4 ± 0.5	3.9 ± 0.7	4.6 ± 0.5	5.6 ± 0.5
P5a	6.8 ± 0.4	6.2 ± 1.1	8.6 ± 0.4	25.5 ± 2.6
P5b	0.28 ± 0.07	>20	0.49 ± 0.22	5.7 ± 1.1
ANF[b]	0.05 ± 0.02	0.04 ± 0.02	>10	>10

[a]All values represent mean and standard deviations (± SD) from three independent experiments. [b]ANF (α-naphthoflavone) was used as a positive control in this experiment.

The results in Table 3 clearly indicate that although ANF is a potent inhibitor of CYP1A1 and CYP1B1, as has been reported before, it does not inhibit CYP1A1 and CYP1B1 enzymes expressed within live HEK293 cells, grown in suspension. One reason for this could be that ANF is highly insoluble[20, 48, 49, 55] and that it precipitates in cell culture media.

2.3. Furanochalcones Pongapin and Lanceolatin B are Selective Inhibitors of CYP1 Sub-family of Enzymes. To understand the selectivity profile, the two best compounds pongapin and lanceolatin B were tested against a panel of 12 human CYP450 enzymes viz. CYP1A1, CYP1A2, CYP1B1, CYP2A6, CYP2B6, CYP2C8, CYP2C9, CYP2C18, CYP2C19, CYP2D6, CYP2E1, and CYP3A4 using Sacchrosomes™. Both pongapin and lanceolatin B manifested the most potent inhibitory activity against CYP1A1 enzyme (with IC_{50} values, 71 and 76 nM, respectively) with lesser inhibitory activity against CYP1B1 and CYP1A2. Amongst the two compounds, pongapin showed excellent selectivity within CYP1 sub-family of enzymes (13 and 35-fold selectivity towards CYP1A1 over CYP1B1 and CYP1A2, respectively) (Table 4). Interestingly, both these compounds do not inhibit CYP2 and CYP3 sub-family of enzymes (IC_{50} $\geq$ 20 µM), indicating their selective inhibition of CYP1 sub-family of enzymes.

Table 4. Profiling of pongapin and lanceolatin B against a panel of CYP1, CYP2 and CYP3 sub-family enzymes, using Sacchrosomes™.

CYP	IC_{50} (µM) ± SD (Sacchrosomes™)[a]	
	Pongapin	**Lanceolatin B**
CYP1A1	0.071 ± 0.008	0.076 ± 0.008
CYP1A2	2.5 ± 0.21	0.187 ± 0.12
CYP1B1	0.95 ± 0.12	0.29 ± 0.07
CYP2A6	>20	>20
CYP2B6	>20	>20
CYP2C8	>20	>20

CYP2C9	>20	>20
CYP2C18	>20	>20
CYP2C19	>20	>20
CYP2D6	>20	>20
CYP2E1	>20	>20
CYP3A4	>20	>20

[a]All values represent mean and standard deviations (± SD) from three independent experiments.

2.4. The Potent CYP1A1 Inhibitors Identified Protect Human CYP1A1-overexpressing HEK293 Cells from B[a]P-mediated Toxicity. The aryl hydrocarbon hydroxylase (CYP1A1) is involved in the metabolic activation of aromatic hydrocarbons. It catalyzes the oxidation of B[a]P to form B[a]P-7,8-epoxide which further oxidizes to B[a]P-7,8-dihydrodiol. With the help of an epoxide hydrolase, B[a]P-7,8-dihydrodiol is finally converted to B[a]P-7,8-dihydrodiol-9,10-epoxide which is a carcinogen. In this study, we took recombinant HEK293 cells that harbor a plasmid that encodes the human *CYP1A1* gene and cells which contained a plasmid without the *CYP1A1* gene (i.e. an empty plasmid).[20, 48, 49] B[a]P causes toxicity (i.e. inhibits cell growth) in both cell types but with different EC_{50} values (i.e. the half maximal inhibitory concentrations relating to block in cell growth). The EC_{50} for cell growth inhibition by B[a]P in HEK293 cells, transfected with the empty plasmid, was found to be 14 ± 1.2 µM; whereas the EC_{50} value of B[a]P is ~10-fold lower in cells (i.e. HEK293::pcDNA3.1/CYP1A1) transfected with the plasmid encoding the human *CYP1* gene cells ($EC_{50} = 1.4 \pm 0.4$). This is because the CYP1A1-mediated metabolic activation of B[a]P produces a toxic metabolite and therefore there is more cellular toxicity that translates to more efficient block in cell growth.

The methanolic extract (ME), three natural products pongamol, pongapin, lanceolatin B and one semisynthetic derivative **P5b** were tested for their ability to rescue human HEK293 cells from B[a]P toxicity. The ME completely rescued human cells from CYP1A1-mediated B[a]P toxicity at 3 x IC_{50} concentration, restoring the EC_{50} value of B[a]P. The furanoflavones, pongapin and lanceolatin B at 0.06 µM concentration (i.e. at 3 x IC_{50}), completely protected human cells from B[a]P toxicity, restoring EC_{50} value of B[a]P to 14.8 and 14.4 μM, respectively. The furanochalcone, pongamol and its derivative **P5b** (at 3 x IC_{50} concentrations) also rescued human cells from B[a]P toxicity but could restore the EC_{50} value of B[a]P only to 10.2 and 12.8 μM, respectively (which is 73 and 91% rescue). Results are shown in Figure 3.
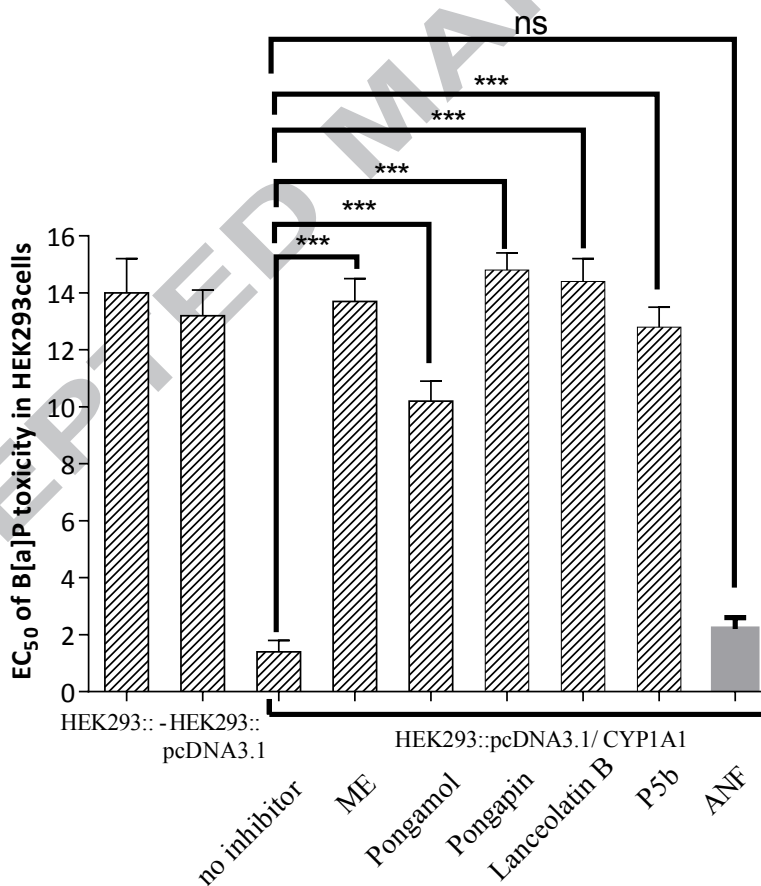

Figure 3. Protection of HEK293 cells from B[a]P toxicity. EC_{50} values of B[a]P after treatment of CYP1A1-overexpressing adherent HEK293 cells with B[a]P and a CYP1A1 inhibitor are plotted. A range

15

of concentrations of B[a]P (0.05 μM – 100 μM) were used, in the presence of 3 x IC_{50} values of the compounds or at 3 x IC_{50} value of ME (as determined in the human cell assay where cells, grown in suspension, expressed CYP1A1). Adherent HEK293 cells were transfected with pcDNA3.1/hCYP1A1 (plasmid encoding the human *CYP1A1* gene). ANF (alpha-naphthoflavone) was used as a positive control in this experiment. All values, presented in μM concentrations, represent the mean and standard deviations of three independent experiments (statistical analysis. ***P < 0.001; ** P < 0.005; * P < 0.01; ns: not significant; P > 0.01).

2.5. Pongapin and Lanceolatin B Block Cell Growth in MCF7-1A1 Cells (i.e. MCF-7 Breast Cancer Cells That Overexpress CYP1A1) at G_0-G_1 Phase of the Cell Cycle and Repress Cyclin D1 Levels. It has been reported that siRNA-mediated knockdown of CYP1A1 inhibits cell proliferation of MCF-7 breast cancer cells blocking cell growth at the G_0-G_1 phase of the cell cycle.[28] However, it was also noted that ANF, a published CYP1A1 inhibitor,[29] does not affect MCF-7 cell proliferation. We have reported earlier that ANF is unable to inhibit potently CYP1A1 enzyme expressed within HEK293 cells;[19, 21, 30] also Table 3 of this paper). We have now confirmed that ANF (50 μM concentration) has no effect on the proliferation of MCF7-1A1 cells (compare Figures 4B and 4C), which stably overexpress CYP1A1 from a plasmid encoding the human *CYP1A1* gene (Figure 4A). ANF's EC_{50} value for inhibition of MCF7-1A1 cell proliferation was determined to be >20 μM. Nevertheless, the methanolic extract (EC_{50} for inhibition of proliferation of MCF7-1A1, 3.8 ± 0.4 μg/mL) from the seeds of *P. pinnata*, and the plant's secondary metabolites pongapin (EC_{50} for inhibition of MCF7-1A1 proliferation, 0.6 ± 0.15 μM), lanceolatin B (EC_{50} for inhibition of MCF7-1A1 proliferation, 0.7 ± 0.12 μM) do block MCF7-1A1 cells at G_0-G_1 (compare Figures 4D, 4E, 4F with 4A) and repress cyclin D1 levels (Figure 4F), when cells were treated with 2x EC_{50} concentration of extract or metabolites. Cyclin dependent kinase-4 (Cdk4), which acts at G_0-G_1, is activated by

cyclin D1. With greatly diminished levels of cyclin D1, Cdk4 is unable to be appropriately active. Hence, because of Cdk4 inactivation, cells probably cannot progress from the G_0-G_1 phase and, thus, cannot proliferate.[56, 57]
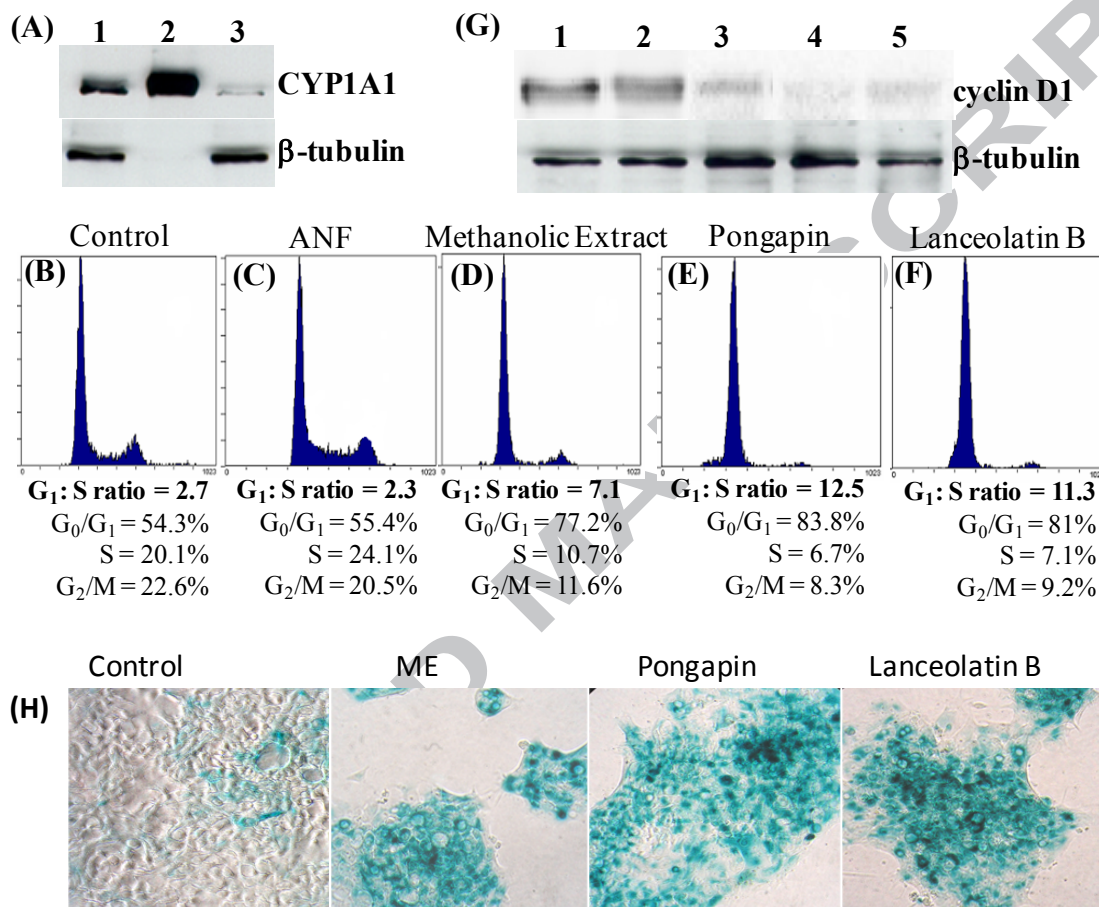

Figure 4.(A-F). Effect of CYP1A1 inhibitors, identified in *P. pinnata* seeds, on the cell division cycle of MCF7-1A1 cells that overexpress CYP1A1. (A): Western blot of MCF7-1A1 cells overexpressing CYP1A1. Lane 1, MCF-7 cells transfected with the plasmid pcDNA3.1/CYP1A1, lane 2, 2 picomoles of CYP1A1-Sacchrosomes™, lane 3, MCF-7 cells transfected with an empty plasmid. (B) to (F): cell cycle analyses (i.e. FACS analyses) of asynchronous MCF7-1A1 cells after treatment, for 24 h, with 2x EC_{50} concentration of compounds [(C), (E) and (F)]and methanolic extract [(D)], or in the absence of any compound or extract [(B)]. (G): Western blot of MCF7-1A1 cells, after treatment with compounds/seed-extract for 24 h, to assess cyclin D1 levels within cells. Lane 1, Control, untreated asynchronous MCF7-1A cells; asynchronous MCF7-1A cells treated with ANF (lane 2), methanolic extract (lane 3), pongapin (lane 4) and lanceolatin B (lane 5). Beta-tubulin was used as a loading control in both Western blots. The CYP1A1, cyclin D1 and β-tubulin-specific antibodies, used for monitoring protein expression, were from

17

ProteinTech (#13241-1-A; CYP1A1), Santa Cruz Biotechnology (#sc-718) and Abcam (#ab6046; β-tubulin). **(H)**. MCF7-1A1 cells showing induction of β-galactosidase, a senescence-associated marker, upon treatment with 2x EC_{50} concentration of *P. pinnata* seed-extract (ME - methanolic extract), pongapin and lanceolatin B. Untreated and treated cells were stained for β-galactosidase activity after 96 h. The stained cells were observed under a phase-contrast microscope (Olympus CKX41) and the percentage of cells expressing β-galactosidase was determined. The blue-stained cells indicate β-galactosidase activity, a marker for senescence.

2.6. Pongapin and Lanceolatin B Induce Senescence in MCF7-1A1 Cells. Cellular inhibition of Cdk4 enzyme, in cancer cells, may induce apoptosis and/or senescence which is a state analogous to terminal differentiation.[58-60] Since our cell cycle analyses (Figures 4B to D) did not show a sub-G1 peak, which is normally indicative of apoptosis, when MCF7-1A1 cells were treated with the seed-extract of *P. pinnata*, and its secondary metabolites pongapin and lanceolatin B, we tested if MCF7-1A1 cells underwent senescence. Senescence is reflected by induction of senescence-associated markers such as neutral β-galactosidase. Interestingly, it was found that the *P. pinnata* seed-extract, pongapin and lanceolatin B do induce β-galactosidase in MCF7-1A1 cells (Figure 4H). Approximately 60-70% cells were positive for β-galactosidase activity out of which more than 20% cells were strongly positive (cells staining dark blue). The control MCF7-1A1 cultures showed less than 10% cells positive for β-galactosidase and were weakly stained (cells stained light blue).

2.7. Molecular Modelling of Pongapin, Lanceolatin B and a Pyrazole Derivative P5b with CYP1A1. The X-ray crystal structure of human CYP1A1 (PDB ID: 4I8V), published in 2013 by Walsh and co-workers [11], was used for this study. Docking of the three inhibitors pongapin, lanceolatin B and a pyrazole derivative **P5b** was carried out using GLIDE module of Schrodinger molecular modeling suite. The docking protocol was validated by re-docking ANF[29]

in the CYP1A1 active site (Figure 5A). The interactions of pongapin, lanceolatin B and pyrazole derivative **P5b**, with the active site residues of CYP1A1, are shown in Figures 5B, 5C and 5D, respectively. Pongapin showed four important H-bonding interactions with Thr 497, Thr 321, Asn 222 and Asp 320 amino acid residues, along with two π-π interactions with Phe 224 and Phe 123 residues. Unlike pongapin, lanceolatin B oriented in the active site of CYP1A1, with furan ring closer to the heme. The carbonyl group of lanceolatin B showed H-bonding interactions with Asn 222 and Thr 497 residues. The chroman and phenyl ring of lanceolatin B showed π-π interactions with Phe 258 and Phe 224 residues. Additionally, the furan ring also displayed π-π interaction with Phe 123 amino acid. Interestingly, the pyrazole derivative **P5b** displayed several additional interactions along with other shared interactions of the three inhibitors. Like lanceolatin B, the furan ring of **P5b** oriented towards the heme. The furan oxygen showed H-bonding with Ile 386. Other H-bonding interactions of **P5b** include the interaction between 1′-N of pyrazole with Thr 321 and Asp 320, and interaction of CN with Thr 497 residue. Apart from these interactions, three hydrophobic π-π interactions were observed with Phe 224, Phe 258 and Phe 319 residues. Docking studies indicated that these identified CYP1A1 inhibitors display strong binding and interactions at the active site of CYP1A1 enzyme.
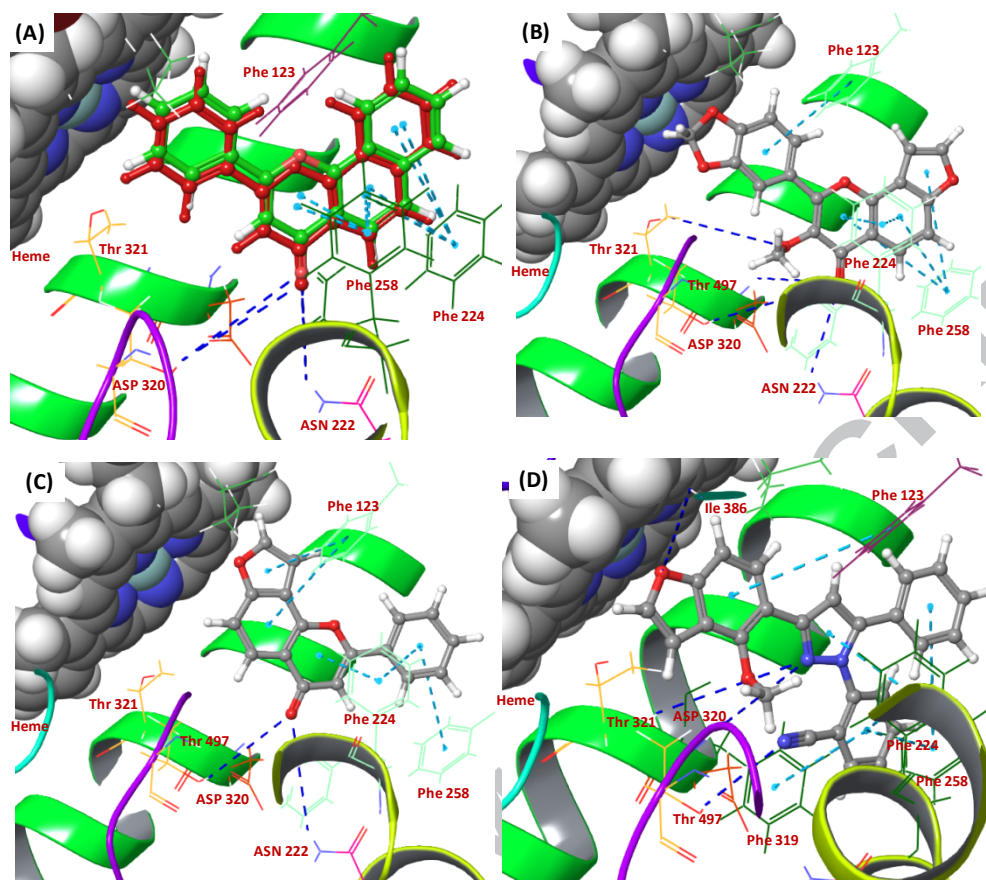
19

Figure 5. Molecular modeling of ANF, pongapin, lanceolatin B and the pyrazole derivative **P5b** with CYP1A1 (PDB: 4I8V). (A) Overlay of ANF on co-crystal crystal structure (red) and docked ANF (green). (B) Interactions of pongapin with CYP1A1. (C) Interactions of lanceolatin B with CYP1A1. (D) Interactions of the pyrazole derivative **P5b** with CYP1A1.

3. CONCLUSIONS

In summary, we have identified that the methanolic extract of *P. pinnata* seeds displays strong inhibition of CYP1 sub-family of enzymes. The two furanoflavone secondary metabolites isolated from *P. pinnata* seeds, pongapin and lanceolatin B, were identified as highly potent and selective inhibitors of CYP1A1 (both having CYP1A1 IC_{50} values of 20 nM in human cells) with little effect on CYP2 and 3 sub-family of enzymes (IC_{50}, >20 µM). The seed-extract, pongapin and lanceolatin B, protect human cells, expressing CYP1A1, from the toxicity of the

procarcinogen B[a]P. We have confirmed earlier findings [28] that the CYP1A1 inhibitor ANF has no effect on the cell division cycle. Surprisingly however, pongapin and lanceolatin B block breast cancer MCF-7 cells, that overexpress CYP1A1, at G_0-G_1 phase of the cell division cycle, with perceptible reduction in cyclin D1 levels. It appears that this early arrest of the cell cycle causes cellular senescence, a yet unreported facet of CYP1A1 inhibition. Thus, the leads identified, herein, have potential for further investigation as potential cancer chemopreventive agents.

4. EXPERIMENTAL SECTION

4.1. General. All chemicals were obtained from Sigma-Aldrich Company and used as received. ^1H, ^{13}C and DEPT NMR spectra were recorded on Bruker-Avance DPX FT-NMR 500 and 400 MHz instruments. Chemical data for protons are reported in parts per million (ppm) downfield from tetramethylsilane and are referenced to the residual proton in the NMR solvent (CDCl$_3$, 7.26 ppm). Carbon nuclear magnetic resonance spectra (^{13}C NMR) were recorded at 125 MHz or 100 MHz: chemical data for carbons are reported in parts per million (ppm, δ scale) downfield from tetramethylsilane and are referenced to the carbon resonance of the solvents (CDCl$_3$: 77.36 ppm). ESI-MS and HRMS spectra were recorded on Agilent 1100 LC-Q-TOF and HRMS-6540-UHD machines. IR spectra were recorded on Perkin-Elmer IR spectrophotometer. Melting points were recorded on digital melting point apparatus. The HPLC analysis was carried out on Shimdzu HPLC system using Chromolith C-18e column (Merck, 4.6 X 2.5 mm) and PDA detector. The authentic plant material *Pongamia pinnata*(L.) Pierre was provided by the biodiversity and applied botany division of Indian Institute of Integrative Medicine (CSIR),

Jammu, from the plain area of the Jammu region of India. A specimen sample (accession number: 22898) was preserved in Janaki Ammal Herbarium at the IIIM (CSIR), Jammu, India

4.2. Extraction and Isolation. Three extracts viz. methanol, hydroalcoholic and chloroform were prepared for activity profiling. For phytochemical investigation, the dried and powdered seeds (2.5 kg) were extracted by cold percolation, with methanol (3 × 2 L), and the combined filtrate was concentrated to afford 1000 g of extract. This extract was suspended in water and sequentially fractionated with different solvents including hexane, ethyl acetate, chloroform, and *n*-butanol yielding 200, 400, 90 and 120 g extracts, respectively. The ethyl acetate fraction (400 g) was subjected to column chromatography using step-gradient system of hexane and ethyl acetate in the range of 3 to 50%, which yielded ten major fractions. The 9th fraction produced karanjin (200 mg), which was obtained in pure form by crystallization in methanol. The 3rd and 4th fraction contained an oily compound, which was subjected to crystallization in methanol to obtain pongamol (350 mg). The 5th and 6th fraction on crystallization in methanol gave ovalitenone (50 mg) as a white powder. The 10th fraction gave the white fluffy compound pongol (200 mg) after silica gel column chromatography. The 7th fraction produced the yellow crystalline compound pongapin (10 mg) which was subjected to crystallization. Isolated compounds karanjin,[20, 61] pongamol,[51, 53, 54] ovalitenone,[51, 62] pongol[63] and pongapin[64] were characterized by comparison of their spectral data with literature values (Section S2, supporting information).

4.3. Synthesis of Lanceolatin B and Pongaglabrone [51]. To the solution of pongamol or ovalitenone (100 mg, 1 equiv.) in DMF was added K_2CO_3 (2 equiv.) and the reaction mixture was stirred at 60 °C for 12 h. After completion of the reaction, the reaction mixture was partitioned between water and dichloromethane. The organic layer was collected and evaporated

in vacuo and the crude product was purified using silica gel column chromatography to obtain lanceolatin B and pongaglabrone, respectively. Both these compounds were characterized by comparison of their spectral data with literature values.[51]

4.4. Synthesis of Oxazole Derivatives P1a and P1b. Pongamol (100 mg, 1 mmol) was dissolved in acetic acid (3 mL) followed by addition of hydroxylamine hydrochloride (28 mg, 1.2 equiv) at 70 °C for 4 h under inert atmosphere. After completion of the reaction, it was concentrated under reduced pressure. The reaction mixture was diluted with chloroform and water was added to the resultant mixture leading to formation of a white precipitate in the aqueous layer. The organic layer was decanted off and the remaining solid residue was washed two times with chloroform. The combined chloroform layer was evaporated under reduced pressure and the residue obtained was purified by silica gel (#100-200) column chromatography using hexane-ethyl acetate as an eluent to yield oxazoles **P1a** and **P1b** in 64% yield (combined yield of isomers).

*4.4.1. 3-(4-Methoxybenzofuran-5-yl)-5-phenylisoxazole (**P1a**).* Viscous brown liquid [31 mg, 32% from pongamol]; HPLC t_R 5.2 min (100% purity); IR (CHCl$_3$) ν_{max} 3385, 3172, 3001, 2989, 2919, 2850, 1883, 1730, 1611, 1590, 1572, 1484, 1456, 1416, 1394 cm^{-1}; ^{1}H NMR (400 MHz, CDCl$_3$) δ (ppm) 7.88-7.86 (m, 3H, CH), 7.63 (d, *J* = 2.2 Hz, 1H, CH-2), 7.51-7.45 (m, 3H, CH), 7.33 (d, *J* = 8.6 Hz, 1H, CH-7), 7.06 (s, 1H, CH-4'), 7.01 (d, *J* = 4.0 Hz, 1H, CH-3), 4.10 (s, 3H, OMe); ^{13}C NMR (100 MHz, CDCl$_3$) δ (ppm) 168.4 (C-5'), 159.8 (C-3'), 156.7 (C-7a), 150.8 (C-4), 143.4 (C-2), 128.9 (C-4"), 127.9 (C-3", C-5"), 126.8 (C-2",C-6"), 124.7 (C-6), 118.2 (C-3a), 113.6 (C-5), 106.0 (C-7), 103.9 (C-3), 99.6 (C-4'), 59.6 (OMe); HR-ESIMS *m/z* 292.0964 [M+H]$^+$ (calcd for C$_{18}$H$_{14}$NO$_3$, 292.0968).

*4.4.2. 5-(4-Methoxybenzofuran-5-yl)-3-phenylisoxazole (**P1b**)*. brown crystalline solid [32 mg, 32% from pongamol]; HPLC t_R 5.4 min (100% purity); mp 107-108 °C; IR (CHCl$_3$) v_{max} 3417, 3018, 2918, 2850, 2099, 1736, 1643, 1605, 1571, 1484, 1467, 1417, 1401, 1352 cm^{-1}; ^{1}H NMR (400 MHz, CDCl$_3$) δ (ppm) 7.96 (d, J = 8.7 Hz, 1H, CH), 7.91 (dd, J = 7.7, 1.5 Hz, 2H, CH), 7.63 (d, J = 2.1 Hz, 1H, CH-2), 7.51-7.46 (m, 3H, CH), 7.31 (d, J = 8.0 Hz, 1H, CH-7), 7.08 (s, 1H, CH-4'), 7.05 (d, J = 1.4 Hz, 1H, CH-3), 4.23 (s, 3H, OMe); ^{13}C NMR (100 MHz, CDCl$_3$) δ (ppm) 167.1 (C-5'), 163.1 (C-3'), 157.9 (C-7a), 151.1 (C-4), 144.7 (C-2), 129.9 (C-3", C-5"), 129.7 (C-2", C-6"), 129.0 (C-1"), 127.0 (C-4") 124.2 (C-6), 118.4 (C-3a), 113.0 (C-5), 106.9 (C-7), 105.4 (C-3), 100.4 (C-4'), 60.1 (OMe); HR-ESIMS *m/z* 292.0953 [M+H]$^+$ (calcd for C$_{18}$H$_{14}$NO$_3$, 292.0968).

4.5. Synthesis of Pyrazole Derivatives P2a-P7a and P1b-P7b. Pongamol (100 mg, 1 mmol) was dissolved in acetic acid (3 mL) followed by addition of substituted phenylhydrazines (1.2 equiv) at 70 °C for 4 h under inert atmosphere. After completion of the reaction, it was concentrated under reduced pressure. The reaction mixture was diluted with chloroform and water was added to the resultant mixture leading to formation of a white precipitate in the aqueous layer. The organic layer was decanted off and the remaining solid residue was washed two times with chloroform. The combined chloroform layer was evaporated under reduced pressure and the residue obtained was purified by silica gel (#100-200) column chromatography using hexane-ethyl acetate as an eluent to yield pyrazoles as a pair of regioisomers **P2a-P7a** and **P1b-P7b** in 52-73% yield (combined yield of isomers). The mixture of regioisomers were separated using semi-preparative HPLC.

*4.5.1. 1-(4-Bromophenyl)-5-(4-methoxybenzofuran-5-yl)-3-phenyl-1H-pyrazole (**P2a**)*. white viscous liquid [52 mg, 34% from pongamol]; HPLC t_R 7.7 min (100% purity); IR (CHCl$_3$)

ν_{max}3584, 3362, 3014, 2921, 2851, 1890, 1731, 1591, 1555, 1537, 1493, 1471, 1461, 1447 cm^{-1};

^{1}H NMR (400 MHz, CDCl$_3$) δ (ppm) 7.93 (d, J = 7.1 Hz, 2H, Ar), 7.60 (d, J = 2.2 Hz, 1H, OC$\underline{H}$=CH), 7.45-7.33 (m, 5H, ArH), 7.26-7.24 (m, 4H, CH), 6.90 (d, J = 2.1 Hz, 1H, OCH=C$\underline{H}$), 6.78 (s, 1H, CH-4'), 3.68 (s, 3H, OMe); ^{13}C NMR (100 MHz, CDCl$_3$) δ(ppm) 157.7 (C-3'), 152.1 (C-7a), 151.0 (C-4), 144.6 (OC$\underline{H}$=CH), 141.7 (C-5'), 140.1 (C-1"), 133.2 (C-1), 132.0 (C-3", C-5"), 128.9 (Ar-3, Ar-5), 128.2 (Ar-4), 127.4 (Ar-2, Ar-6), 126.0 (C-4"), 125.2 (C-2", C-6"), 120.3 (C-6), 118.4 (C-3a), 115.3 (C-5), 106.9 (OCH=$\underline{C}$H), 106.3 (CH-4'), 106.4 (CH-7), 59.2 (OMe); HR-ESIMS m/z 445.0539 [M+H]$^+$ (calcd for C$_{24}$H$_{18}$BrN$_2$O$_2$, 445.0546).

4.5.2. 2-(4-Bromophenyl)-5-(4-methoxybenzofuran-5-yl)-3-phenyl-2H-pyrazole (**P2b**). White powder [50 mg, 33% from pongamol]; HPLC t_R 8.7 min (100% purity); mp 134-136 ºC; IR (CHCl$_3$): ν_{max} 3386, 2918, 2850, 1737, 1589, 1548, 1491, 1420, 1361, 1337, 1257, 1218, 1180 cm^{-1}; ^{1}H NMR (400 MHz, CDCl$_3$) δ (ppm) 8.01 (d, J = 8.6 Hz, 1H, CH), 7.60 (d, J = 2.2 Hz, 1H, OC$\underline{H}$=CH), 7.47-7.46 (d, J = 8.7 Hz, 2H, CH), 7.36 (m, 3H, CH), 7.31 (m, 5H, CH), 7.07 (s, 1H, CH-4') 6.99 (d, J = 1.4 Hz, 1H, OCH=C$\underline{H}$), 4.10 (s, 3H, OMe); ^{13}C NMR (100 MHz, CDCl$_3$): δ (ppm) 156.7 (C-7a), 151.2 (C-5'), 149.6 (C-4), 144.2 (OC$\underline{H}$=CH), 143.6 (C-3′), 139.2 (C-1"), 132.0 (C-3", C-5"), 130.2 (C-1), 128.8 (Ar-3, Ar-5), 128.6 (Ar-4), 128.4 (Ar-2, Ar-6), 126.5 (C-4"), 125.3 (C-2", C-6"), 120.7 (C-6), 119.5 (C-3a), 118.4 (C-5), 109.1 (OCH=$\underline{C}$H), 106.9 (CH-4'), 104.9 (CH-7), 60.5 (OMe); HR-ESIMS m/z 445.0523 [M+H]$^+$ (calcd for C$_{24}$H$_{18}$BrN$_2$O$_2$, 445.0546).

4.5.3. 5-(4-Methoxybenzofuran-5-yl)-2-(perfluorophenyl)-3-phenyl-1H-pyrazole (**P3a**). Brown sticky liquid [48 mg, 31% from pongamol]; HPLC t_R 6.3 min (100% purity); IR (CHCl$_3$) ν_{max} 3584, 3385, 2918, 2850, 1737, 1614, 1532, 1515, 1470, 1422 cm^{-1}; ^{1}H NMR (400 MHz, CDCl$_3$) δ (ppm) 7.90 (d, J = 7.2 Hz, 2H, CH), 7.60 (d, J = 2.2 Hz, 1H, OC$\underline{H}$=CH), 7.45-7.43 (m,

3H, CH), 7.26 (m, 2H, Ar-H), 6.89 (d, 1H, J = 2.2 Hz, OCH=C<u>H</u>), 6.85 (s, 1H, CH-4'), 3.85 (s, 3H, OMe); ^{19}F NMR (376.5 Hz, CDCl$_3$) δ (ppm) -144.90 to -144.94 (d, 2F), -152.98 (s, 1F), -161.74 to -161.75 (d, 2F); ^{13}C NMR (100 MHz, CDCl$_3$) δ (ppm) 161.7 (C-2", C-6") , 157.4 (C-3'), 154.0 (C-7a), 152.9 (C-4"), 150.8 (C-4), 144.9 (C-3", C-5"), 144.8 (C-5′), 144.5 (O<u>C</u>H=CH), 132.2 (Ar-1), 128.6 (Ar-3, Ar-5), 128.3 (Ar-4), 126.8 (Ar-2, Ar-6), 125.8 (C-6), 118.3 (C-3a), 118.1 (C-5), 113.6 (C-1"), 106.4 (C-4′), 106.4 (OCH=<u>C</u>H), 104.8 (C-7), 59.8 (OMe); HR-ESIMS m/z 457.0961 [M+H]$^+$ (calcd for C$_{24}$H$_{14}$F$_5$N$_2$O$_2$, 457.0970).

4.5.4. 5-(4-Methoxybenzofuran-5-yl)-2-(perfluorophenyl)-3-phenyl-2H-pyrazole **(P3b)**. White crystalline solid [45 mg, 29% from pongamol]; HPLC t_R 6.6 min (100% purity); mp 157-159 ºC; IR (CHCl$_3$) ν$_{max}$ 3427, 2919, 2851, 2088, 1642, 1529, 1516, 1465, 1340, 1215, 1080 cm^{-1}; ^{1}H NMR (400 MHz, CDCl$_3$) δ (ppm) 7.93 (d, J = 8.7 Hz, 1H, CH), 7.60 (d, J = 2.2 Hz, 1H,OC<u>H</u>=CH), 7.38 (m, 3H, CH), 7.31 (m, 3H, CH), 7.13 (s, 1H, CH-4′), 7.00 (d, J = 1.4 Hz, 1H, OCH=C<u>H</u>), 4.11 (s, 3H, OMe); ^{19}F NMR (376.5 Hz, CDCl$_3$) δ (ppm) -144.45 to -144.50 (d, 2F), -152.05 (s, 1F), -160.98 to -161.00 (d, 2F); ^{13}C NMR (100 MHz, CDCl$_3$) δ (ppm) 161.0 (2", C-6"), 157.0 (C-7a), 152.0 (C-4"), 152.0 (C-4), 151.5 (C-5'), 144.4 (C-3", C-5"), 147.1 (C-3′), 144.2 (O<u>C</u>H=CH), 129.3 (Ar-3, Ar-5), 129.1 (Ar-1), 128.8 (Ar-4), 127.7 (Ar-2, Ar-6), 125.4 (C-6), 119.5 (C-3a), 118.9 (C-5), 117.8 (C-1′′), 108.0 (C-4′), 106.9 (C-7), 104.9 (OCH=<u>C</u>H), 60.5 (OMe); HR-ESIMS m/z 457.0959 [M+H]$^+$ (calcd for C$_{24}$H$_{14}$F$_5$N$_2$O$_2$, 457.0970).

*4.5.5. 5-(4-Methoxybenzofuran-5-yl)-1-(2-nitrophenyl)-3-phenyl-1H-pyrazole (**P4a**).* yellow viscous liquid [48 mg, 34% from pongamol]; HPLC t_R 5.7 min (100% purity); IR (CHCl$_3$) ν$_{max}$ 3584, 3402, 3019, 2919, 1736, 1615, 1533, 1469, 1348 cm^{-1}; ^{1}H NMR (400 MHz, CDCl$_3$) δ (ppm) 8.38 (t, J = 2.0 Hz, 1H, CH), 8.07 (dd, J = 8.2, 1.2 Hz, 1H, CH), 7.95 (d, J = 7.2 Hz, 2H, CH), 7.63 (d, J = 2.2 Hz, 1H, OC<u>H</u>=CH), 7.61 (d, J = 8.2 Hz, 1H, CH), 7.45-7.37 (m, 4H, CH),

26

7.30 (m, 2H, CH), 6.88 (d, J = 2.2 Hz, 1H, OCH=C$\underline{H}$), 6.82 (s, 1H, CH-4′), 3.71 (s, 3H, OMe);

^{13}C NMR (100 MHz, CDCl$_3$) δ (ppm) 157.7 (C-7a), 152.6 (C-4), 150.7 (C-3′), 148.3 (C-5′),

144.6 (OC$\underline{H}$=CH), 141.9 (C-2′′), 141.8 (C-1′′), 132.6 (Ar-1), 129.3 (C-5′′), 128.7 (Ar-3, Ar-5),

128.6 (Ar-4), 128.3 (C-3′′), 127.0 (C-4′′), 125.8 (Ar-2, Ar-6), 121.1 (C-6), 118.4 (C-6′′), 118.2

(C-3a), 114.6 (C-5), 107.4 (C-4′), 106.4 (C-7), 105.0 (OCH=C$\underline{H}$), 59.4 (OMe); HR-ESIMS m/z

412.1285 [M+H]$^+$ (calcd for C$_{24}$H$_{18}$N$_3$O$_4$, 412.1291).

*4.5.6. 5-(4-Methoxybenzofuran-5-yl)-2-(2-nitrophenyl)-3-phenyl-2H-pyrazole **(P4b)**.* yellow

sticky solid [54 mg, 39% from pongamol]; HPLC t_R 6.2 min (100% purity); IR (CHCl$_3$) ν$_{max}$

3584, 2918, 2850, 1737, 1613, 1590, 1531, 1502, 1475, 1432, 1413, 1339, 1351, 1256, 1180 cm$^-$

^{1}; ^{1}H NMR (400 MHz, CDCl$_3$) δ (ppm) 8.36 (t, J = 2.0 Hz, 1H, CH), 8.13 (dd, J = 8.2, 1.2 Hz,

1H, CH-3′′), 8.04 (d, J = 8.6 Hz, 1H, CH), 7.66 (d, J = 8.0 Hz, 1H, CH), 7.61 (d, J = 2.2 Hz, 1H,

OC$\underline{H}$=CH), 7.48 (t, J = 8.1 Hz, 1H, CH), 7.36-7.32 (m, 6H, CH), 7.11 (s, 1H, CH-4'), 7.00 (d, J

= 1.4 Hz, 1H, OCH=C$\underline{H}$), 4.12 (s, 3H, OMe); ^{13}C NMR (100 MHz, CDCl$_3$) δ (ppm) 156.9 (C-6),

151.4 (C-4), 150.4 (C-5′), 148.4 (C-3′), 144.3 (OC$\underline{H}$=CH), 143.9 (C-2′′) 141.1 (C-1′′), 130.2 (

C-5′′), 130.2 (Ar-1), 129.5 (C-4′′), 128.9 (Ar-3, Ar-5), 128.7 (Ar-4), 128.8 (Ar-2, Ar-6), 125.3

(C-3′′), 121.4 (C-6), 119.6 (C-6′′), 119.4 (C-3a), 117.9 (C-5), 109.9 (C-4′), 107.0 (C-7), 104.9

(OCH=C$\underline{H}$), 60.5 (OMe); HR-ESIMS m/z 412.1287 [M+H]$^+$ (calcd for C$_{24}$H$_{18}$N$_3$O$_4$, 412.1291).

*4.5.7. 4-(5-(4-Methoxybenzofuran-5-yl)-3-phenyl-1H-pyrazol-1-yl)benzonitrile **(P5a)***.

white powder [44 mg, 33% from pongamol]; HPLC t_R 4.2 min (100% purity); mp 140-146 ºC;

IR (CHCl$_3$): ν$_{max}$ 3584, 3420, 3040, 2900, 2840, 2200, 1600, 1510, 1474, 1410, 1364, 1217,

1064 cm^{-1}; ^{1}H NMR (400 MHz, CDCl$_3$) δ (ppm) 7.93 (d, J = 7.2 Hz, 2H, CH), 7.62 (d, J = 2.2

Hz, 1H, OC$\underline{H}$=CH), 7.56 (d, J = 8.7 Hz, 2H, CH), 7.49-7.43 (m, 4H, CH), 7.38 (d, J = 7.3 Hz,

1H, CH), 7.30 (s, 2H, CH), 6.90 (d, J = 2.2 Hz, 1H, OCH=C$\underline{H}$), 6.81 (s, 1H, CH- 4′), 3.67 (s,

27

3H, OMe); ^{13}C NMR (100 MHz, CDCl$_3$) δ (ppm) 156.9 (C-7a), 151.4 (C-4), 150.6 (C-3'), 144.2 (OCH=CH), 143.9 (C-5'), 143.5 (C-1''), 132.8 (C-3''), 130.4 (Ar-1), 128.9 (Ar-3, Ar-5), 128.6 (Ar-4), 128.7 (Ar-2, Ar-6), 125.8 (C-5''), 125.3 (C-4''), 124.6 (C-6''), 123.1 (C-6), 119.4 (C-3a), 118.4 (C-5), 117.9 (C≡N), 110.4 (C-2''), 110.1 (C-4'), 106.9 (OCH=CH), 104.9 (C-7), 60.4 (OMe); HR-ESIMS *m/z* 392.1380 [M+H]$^+$ (calcd for C$_{25}$H$_{18}$N$_3$O$_2$, 392.1393).

*4.5.8. 4-(5-(4-Methoxybenzofuran-5-yl)-3-phenyl-2H-pyrazol-2-yl)benzonitrile (**P5b**)*. white powder [47 mg, 35% from pongamol]; HPLC t_R 4.7 min (100% purity); mp 139-140 ^{o}C; IR (CHCl$_3$) ν_{max} 3584, 3402, 2955, 2918, 2850, 2228, 1737, 1606, 1511, 1465, 1422, 1362, 1339, 1219 cm^{-1}; ^{1}H NMR (400 MHz, CDCl$_3$): δ (ppm) 8.03 (d, *J* = 8.6 Hz, 1H, CH), 7.61 (d, *J* = 1.4 Hz, 1H, OCH=CH), 7.60 (d, *J* = 4.0 Hz, 2H, CH), 7.52 (d, *J* = 8.6 Hz, 2H, CH), 7.40 (dd, *J* = 5.0, 1.6 Hz, 3H, CH), 7.32 (m, 3H, CH), 7.09 (s, 1H, CH-4'), 6.99 (d, *J* = 1.4 Hz, 1H, OCH=CH), 4.11 (s, 3H, OMe); ^{13}C NMR (100 MHz, CDCl$_3$) δ (ppm) 156.7 (C-7a), 151.0 (C-4), 149.7 (C-5'), 144.1 (OCH=CH), 143.8 (C-3'), 143.3 (C-1''), 132.7 (C-3''), 130.1 (Ar-1), 128.7 (Ar-3, Ar-5), 128.7 (Ar-2, Ar-6), 128.6 (Ar-4), 125.5 (C-5''), 125.1 (C-4''), 124.7 (C-6''), 123.5 (C-6), 119.1 (C-3a), 118.1 (C-5), 117.7 (C≡N), 110.2 (C-2''), 110.1 (C-4'), 106.8 (OCH=CH), 105.8 (C-7), 60.5 (OMe); HR-ESIMS *m/z* 392.1380 [M+H]$^+$ (calcd for C$_{25}$H$_{18}$N$_3$O$_2$, 392.1393).

*4.5.9. 1-(2-Chlorophenyl)-5-(4-methoxybenzofuran-5-yl)-3-phenyl-1H-pyrazole (**P6a**)*. viscous brown liquid [46 mg, 34% from pongamol]; HPLC t_R 7.3 min (100% purity); IR (CHCl$_3$) ν_{max} 3382, 3063, 2918, 2850, 1889, 1733, 1594, 1555, 1496, 1470, 1447 cm^{-1}; ^{1}H NMR (400 MHz, CDCl$_3$) δ (ppm) 7.93 (d, *J* = 7.2 Hz, 2H, CH), 7.60 (d, *J* = 2.2 Hz, 1H, OCH=CH), 7.45 (t, *J* = 7.5 Hz, 2H, CH), 7.33 (m, 3H, CH), 7.26 (m, 4H, CH), 6.89 (d, *J* = 2.2 Hz, 1H, OCH=CH), 6.78 (s, 1H, CH-4'), 3.68 (s, 3H, OMe); ^{13}C NMR (100 MHz, CDCl$_3$) δ (ppm) 157.5 (C-7a), 152.0 (C-4), 150.9 (C-3'), 144.4 (OCH=CH), 141.4 (C-5'), 139.5 (C-1''), 133.1 (Ar-1),

28

132.3 (C-4´´), 128.7 (Ar-3, Ar-5), 128.6 (Ar-4), 128.0 (Ar-2, Ar-6), 127.2 (C-3´´, C-5´´), 125.8 (C-6), 124.7 (C-2´´, C-6´´), 118.3 (C-3a), 115.2 (C-5), 106.7 (C-4´), 106.1 (C-7), 106.1 (OCH=$\underline{C}$H)), 59.3 (OMe); HR-ESIMS *m/z* 401.1050 [M+H]$^+$ (calcd for $C_{24}H_{18}ClN_2O_2$, 401.1051).

4.5.10.   2-(2-Chlorophenyl)-5-(4-methoxybenzofuran-5-yl)-3-phenyl-2H-pyrazole (**P6b**). crystalline solid [42 mg, 31% from pongamol]; HPLC t_R 8.2 min (100% purity); mp 151-153 ᵒC; IR (CHCl₃) ν$_{max}$ 3429, 3018, 2919, 2850, 2095, 1732, 1639, 1549, 1495, 1473, 1421, 1362, 1337, 1217, 1180, 1153, 1093 cm^{-1}; ^{1}H NMR (400 MHz, CDCl₃) δ (ppm) 8.02 (d, *J* = 8.6 Hz, 1H, CH), 7.60 (d, *J* = 2.2 Hz, 1H, OC$\underline{H}$=CH), 7.36 (m, 3H, CH), 7.32 (m, 7H, CH), 7.07 (s, 1H, CH-4´), 6.99 (d, *J* = 1.4 Hz, 1H, OCH=C$\underline{H}$), 4.10 (s, 3H, OMe); ^{13}C NMR (100 MHz, CDCl₃) δ (ppm) 156.8 (C-7a), 151.3 (C-4), 149.6 (C-5´), 144.1 (O$\underline{C}$H=CH), 143.6 (C-3´), 138.8 (C-1´´), 132.8 (Ar-1), 130.7 (C-4´´), 129.0 (Ar-3, Ar-5), 128.8 (Ar-4), 128.6 (Ar-2, Ar-6), 128.3 (C-3´´, C-5´´), 126.2 (C-6), 125.4 (C-2´´, C-6´´), 119.6 (C-3a), 118.5 (C-5), 109.0 (C-4´), 106.9 (C-7), 104.1 (OCH=$\underline{C}$H), 60.4 (OMe); HR-ESIMS *m/z* 401.1035 [M+H]$^+$ (calcd for $C_{24}H_{18}ClN_2O_2$, 401.1051).

4.5.11. 1-(2,4-Dichlorophenyl)-5-(4-methoxybenzofuran-5-yl)-3-phenyl-1H-pyrazole (**P7a**). crystalline solid [38 mg, 26% from pongamol]; HPLC t_R 7.17 min (100% purity); IR (CHCl₃) ν$_{max}$ 3584, 3384, 3066, 2918, 2850, 1736, 1592, 1555, 1490, 1470, 1440, 1428, 1348 cm^{-1}; ^{1}H NMR (400 MHz, CDCl₃) δ (ppm) 7.93 (d, *J* = 7.2 Hz, 2H, CH), 7.57 (d, *J* = 2.2 Hz, 1H, OC$\underline{H}$=CH), 7.42 (m, 3H, CH), 7.33 (m, 3H, CH), 7.20 (m, 3H, CH), 6.89 (d, *J* = 2.1 Hz, 1H, OCH=C$\underline{H}$), 6.82 (s, 1H, CH-4´), 3.87 (s, 3H, OMe); ^{13}C NMR (100 MHz, CDCl₃) δ (ppm) 157.3 (C-7a), 152.4 (C-4), 150.9 (C-3´), 144.3 (O$\underline{C}$H=CH), 143.2 (C-5´), 137.2 (C-1´´), 134.6 (C-2´´), 133.0 (C-4´´), 132.8 (Ar-1), 130.3 (C-3´´), 130.1 (C-5´´), 128.6 (Ar-3, Ar-5), 128.0 (Ar-4), 127.3

(Ar-2, Ar-6), 127.2 (C-6''), 125.8 (C-6), 118.0 (C-3a), 114.6 (C-5), 105.9 (C-4'), 105.5 (C-7), 105.1 (OCH=$\underline{C}$H), 59.6 (OMe); HR-ESIMS m/z 435.0654 [M+H]$^+$ (calcd for $C_{24}H_{17}Cl_2 N_2O_2$, 435.0661).

4.5.12. 2-(2,4-Dichlorophenyl)-5-(4-methoxybenzofuran-5-yl)-3-phenyl-2H-pyrazole (**P7b**). Crystalline solid [31 mg, 27% from pongamol]; HPLC t_R 7.19 min (100% purity); mp 157-159 °C; IR (CHCl$_3$) ν_{max} 3443, 2918, 2850, 2095, 1732, 1639, 1549, 1495, 1473, 1421, 1362, 1337, 1217, 1180, 1153, 1093 cm^{-1}; ^{1}H NMR (400 MHz, CDCl$_3$) δ (ppm) 7.98 (d, J = 8.6 Hz, 1H, CH), 7.59 (d, J = 2.2 Hz, 1H, OC$\underline{H}$=CH), 7.46 (m, 2H, CH), 7.32 (m, 5H, CH), 7.27 (d, J = 4.0 Hz, 1H, CH), 7.12 (s, 1H, CH-4'), 6.98 (d, J = 1.4 Hz, 1H, OCH=C$\underline{H}$), 4.10 (s, 3H, OMe); ^{13}C NMR (100 MHz, CDCl$_3$) δ (ppm) 157.4 (C-7a), 152.4 (C-4), 150.9 (C-5'), 144.3 (O$\underline{C}$H=CH), 143.3 (C-3'), 137.2 (C-1''), 134.7 (C-2''), 133.1 (C-4''), 132.8 (Ar-1), 130.3 (C-3''), 130.1 (C-5''), 128.6 (Ar-3, Ar-5), 128.0 (Ar-4), 127.3 (Ar-2, Ar-6), 127.2 (C-6''), 125.9 (C-6), 118.1 (C-3a), 114.7 (C-5), 105.9 (C-4'), 105.5 (C-7), 105.1 (OCH=$\underline{C}$H)), 59.7 (OMe); HR-ESIMS m/z 435.0660 [M+H]$^+$ (calcd for $C_{24}H_{17}Cl_2 N_2O_2$, 435.0661).

4.6. CYP inhibition. The CYP Screening using Sacchrosomes^{TM} and Recombinant Human HEK293 Cells was carried out as described earlier.[20, 48, 49] Similarly, the protection from B[a]P toxicity in CYP1A1-expressing normal adherent human cells was performred using our published protocols.[19, 20, 48]

4.7. Construction of the Stable MCF7-10A Cell Line. After transfection of MCF-7 cells (ATCC # HTB-22) with the CYP1A1 gene-bearing pcDNA3.1 plasmid (i.e. pcDNA3.1/CYP1A1) [49], using the Amaxa-Nucleofector (following the manufacturer's protocols), and the transfectants were seeded onto a 100-mm tissue culture dish (Corning) containing 8 mL of pre-warmed culture medium. After incubation for 2 days, the transfected

cells were selected for G418 resistance in medium containing 1 mg/mL G418 (Gibco/BRL Life Technologies). After 10-15 days, the surviving single colonies (G418-resistant colonies)were picked using cloning rings and transferred to 24-well dishes with further selection in medium containing 200 mg/mL G418. The expression of CYP enzymes, in G418-stabilized transfectants, were determined using Western blotting, enzyme assay using the fluorogenic substrate, 7-ethoxyresorufin. The homogeneity of the transfectants was assured by repeated subcloning.

4.8. In Vitro Cell Proliferation Assays and Flow Cytometric Analyses. This assay was performed as described earlier [65]. Control cells (i.e. in the absence of any compound) and cells (i.e. treated with compound) cells were harvested after treatment with trypsin. Cells were fixed in chilled (-20 ºC) 70% ethanol for an hour, after washing once with PBS. Fixed cells were centrifuged at room temperature. Pellets were re-suspended in PBS, in the presence of DNase-free ribonuclease (0.5 mg/mL; Sigma-Aldrich # R-5503) before staining with a propidium iodide solution (50 μg/mL; Sigma-Aldrich, # P-4170) for an hour (in the dark) at 4 °C. Cell cycle analysis was performed on the Beckman Coulter (Epics Altra) fluorescence-activated cell sorter (Beckman Coulter UK Ltd). To exclude cell doublets or cell clumps, all events that represent single cells were gated. Cytograms of the fluorescence peak of propidium iodide were plotted against the integrated fluorescence/linear signal. Data points on a straight line, within a single gate, were isolated and the gated data was employed for plotting a histogram that represents a complete cell cycle. The total number of events did not exceed 200 events per second. Data acquisition was stopped after collection of around 10,000 events.

4.9. Senescence Assay for Expression of β-Galactosidase. Senescent cells can no longer replicate because they cannot enter the normal cell cycle and undergo cellular mitosis (i.e. senescent cells cannot divide). Senescence, associated with changes in cellular gene expression

patterns, results in the expression of β-galactosidase activity which can be assessed by staining the cells [66, 67]. MCF7-1A1 cells (25,000 cells/well) were seeded in 6-well plates in 2 ml complete growth medium. Cells were incubated for 24 h (to allow for stabilization) followed by 96 h of treatment with test compound or extract (at IC_{50} concentrations). After compound/extract treatment, the growth medium was removed by aspiration and the cells were washed twice with 1 ml PBS. 1.5 ml of fixation buffer was added to each well and the plates were incubated at room temperature for 10 min. While cells were being fixed, the staining mixture was prepared. Cells were washed 3 times with 1 ml PBS and 1 ml of staining mixture was added to each well. The plates were incubated at 37 °C, without CO_2, for 48 h. The cells were observed under the microscope and the percentage of cells expressing β-galactosidase was determined.

4.10. Molecular Modeling. The crystal structure of CYP1A1 (PDB ID: 4I8V)[11] was retrieved from the protein data bank and subjected to protein preparation wizard facility under default conditions, implemented in Maestro v9.0 and Impact program v5.5 (Schrodinger, Inc., New York, NY, 2009). The prepared protein was further utilized to construct grid file by selecting co-crystallized ligand as centroid of grid box. For standardization of molecular docking procedure, co-crystallized ligand such as ANF (a CYP1A1 inhibitor)[29] was extracted from prepared enzyme-ligand complex and re-docked to the CYP1A1 binding site. The rest of the chemical structures were sketched, minimized and docked using GLIDE XP. The ligand-protein complexes were minimized using macromodel. The validation of the docking protocol was done by re-docking the co-crystallized ligand from the protein (4I8V). The overlay of co-crystallized ligand and re-docked ligand is shown in section S6 of the supporting information.

Supporting information. Spectral data scans and X-ray crystallography data.

5. REFERENCES

1. WHO guidelines for indoor air quality: selected pollutants, The WHO European Centre for Environment and Health, Bonn Office [ISBN 978 92 890 0213 4]2010.

2. Ohura T, Amagai T, Fusaya M, et al., Polycyclic aromatic hydrocarbons in indoor and outdoor environments and factors affecting their concentrations, *Environ. Sci. Technol.*, 2004; 38: 77-83.

3. Androutsopoulos VP, Tsatsakis AM, Spandidos DA, Cytochrome P450 CYP1A1: wider roles in cancer progression and prevention, *BMC cancer*, 2009; 9: 187.

4. Kawajiri K, Fujii-Kuriyama Y, Cytochrome P450 gene regulation and physiological functions mediated by the aryl hydrocarbon receptor, *Arch. Biochem. Biophys.*, 2007; 464: 207-212.

5. Ma Q, Induction of CYP1A1. The AhR/DRE paradigm: transcription, receptor regulation, and expanding biological roles, *Curr. Drug Metab.*, 2001; 2: 149-164.

6. Whitlock JP, Jr., Induction of cytochrome P4501A1, *Annu. Rev. Pharmacol. Toxicol.*, 1999; 39: 103-125.

7. Arlt VM, Krais AM, Godschalk RW, et al., Pulmonary inflammation impacts on CYP1A1-mediated respiratory tract DNA damage induced by the carcinogenic air pollutant benzo[a]pyrene., *Toxicol. Sci.*, 2015; 146: 213-225.

8. Beresford AP, CYP1A1: friend or foe?, *Drug. Metab. Rev.* , 1993; 25: 503-517.

9. Smit E, Souza T, Jennen DGJ, et al., Identification of essential transcription factors for adequate DNA damage response after benzo(a)pyrene and aflatoxin B1 exposure by combining transcriptomics with functional genomics, *Toxicology*, 2017; 390: 74-82.

10. Rendic S, Guengerich FP, Contributions of human enzymes in carcinogen metabolism, *Chem. Res. Toxicol.*, 2012; 25: 1316-1383.

11. Walsh AA, Szklarz GD, Scott EE, Human cytochrome P450 1A1 structure and utility in understanding drug and xenobiotic metabolism, *J. Biol. Chem.*, 2013; 288: 12932-12943.

12. Gary JK, Ernest TH, Caroline CS, Cancer chemoprevention. *In Strategies for cancer chemopervention*, Totowa Humana press: New Jersey2005.

13. Stoner G, Morse M, Kelloff G, Perspectives in cancer chemoprevention, *Environ. Health. Perspect.*, 1997; 105: 945-954.

14. Liu J, Taylor SF, Dupart PS, et al., Pyranoflavones: a group of small-molecule probes for exploring the active site cavities of cytochrome P450 enzymes 1A1, 1A2, and 1B1, *J. Med. Chem.*, 2013; 56: 4082-4092.

15. Shiizaki K, Ohsako S, Kawanishi M, et al., Omeprazole alleviates benzo[a]pyrene cytotoxicity by inhibition of CYP1A1 activity in human and mouse hepatoma cells, *Basic Clin. Pharmacol. Toxicol.*, 2008; 103: 468-475.

16. Shiizaki K, Kawanishi M, Yagi T, Modulation of benzo[a]pyrene-DNA adduct formation by CYP1 inducer and inhibitor, *Genes Environ.*, 2017; 39: 14.

17. Chang TK, Chen J, Yang G, et al., Inhibition of procarcinogen-bioactivating human CYP1A1, CYP1A2 and CYP1B1 enzymes by melatonin, *J. Pineal Res.*, 2010; 48: 55-64.

18. Olguin-Reyes S, Camacho-Carranza R, Hernandez-Ojeda S, et al., Bergamottin is a competitive inhibitor of CYP1A1 and is antimutagenic in the Ames test, *Food Chem. Toxicol.*, 2012; 50: 3094-3099.

19. Horley NJ, Beresford KJM, Kaduskar S, et al., (E)-3-(3,4,5-Trimethoxyphenyl)-1-(pyridin-4-yl)prop-2-en-1-one, a heterocyclic chalcone is a potent and selective CYP1A1

inhibitor and cancer chemopreventive agent, *Bioorg. Med. Chem. Lett.*, 2017; 27: 5409-5414.

20. Joshi P, McCann GJP, Sonawane VR, et al., Identification of potent and selective CYP1A1 inhibitors via combined ligand and structure-based virtual screening and their in vitro validation in sacchrosomes and live human cells, *J. Chem. Inf. Model.*, 2017; 57: 1309-1320.

21. Williams IS, Joshi P, Gatchie L, et al., Synthesis and biological evaluation of pyrrole-based chalcones as CYP1 enzyme inhibitors, for possible prevention of cancer and overcoming cisplatin resistance, *Bioorg. Med. Chem. Lett.*, 2017; 27: 3683-3687.

22. Murray GI, Patimalla S, Stewart KN, et al., Profiling the expression of cytochrome P450 in breast cancer, *Histopathology*, 2010; 57: 202-211.

23. Vinothini G, Nagini S, Correlation of xenobiotic-metabolizing enzymes, oxidative stress and NFkappaB signaling with histological grade and menopausal status in patients with adenocarcinoma of the breast, *Clin. Chim. Acta*, 2010; 411: 368-374.

24. Chua MS, Kashiyama E, Bradshaw TD, et al., Role of Cyp1A1 in modulation of antitumor properties of the novel agent 2-(4-amino-3-methylphenyl)benzothiazole (DF 203, NSC 674495) in human breast cancer cells, *Cancer Res.*, 2000; 60: 5196-5203.

25. Trapani V, Patel V, Leong CO, et al., DNA damage and cell cycle arrest induced by 2-(4-amino-3-methylphenyl)-5-fluorobenzothiazole (5F 203, NSC 703786) is attenuated in aryl hydrocarbon receptor deficient MCF-7 cells, *Br. J. Cancer*, 2003; 88: 599-605.

26. Bradshaw TD, Stevens MF, Westwell AD, The discovery of the potent and selective antitumour agent 2-(4-amino-3-methylphenyl)benzothiazole (DF 203) and related compounds, *Curr. Med. Chem.*, 2001; 8: 203-210.

27. Nandekar PP, Sangamwar AT, Cytochrome P450 1A1-mediated anticancer drug discovery: in silico findings, *Expert Opin. Drug Discov.*, 2012; 7: 771-789.

28. Rodriguez M, Potter DA, CYP1A1 regulates breast cancer proliferation and survival, *Mol. Cancer Res.*, 2013; 11: 780-792.

29. Taura K, Naito E, Ishii Y, et al., Cytochrome P450 1A1 (CYP1A1) inhibitor alpha-naphthoflavone interferes with UDP-glucuronosyltransferase (UGT) activity in intact but not in permeabilized hepatic microsomes from 3-methylcholanthrene-treated rats: possible involvement of UGT-P450 interactions, *Biol. Pharm. Bull.*, 2004; 27: 56-60.

30. Sharma R, Gatchie L, Williams IS, et al., Glycyrrhiza glabra extract and quercetin reverses cisplatin resistance in triple-negative MDA-MB-468 breast cancer cells via inhibition of cytochrome P450 1B1 enzyme, *Bioorganic & medicinal chemistry letters*, 2017; 27: 5400-5403.

31. Ayyanar M, Ignacimuthu S, Herbal medicines for wound healing among tribal people in southern india: ethnobotanical and scientific evidences, *Int. J. Appl. Res. Nat. Prod.*, 2009; 2: 29-42.

32. Badole SL, Bodhankar SL, Investigation of antihyperglycaemic activity of aqueous and petroleum ether extract of stem bark of *Pongamia pinnata* on serum glucose level in diabetic mice, *J. Ethnopharmacol.*, 2009; 123: 115-120.

33. Bhatia G, Puri A, Maurya R, et al., Anti-dyslipidemic and antioxidant activities of different fractions of *Pongamia pinnata* (lin.) fruits, *Med. Chem. Res.*, 2008; 17: 618-620.

34. Ranga RR, Tiwari AK, Prabhakar P, et al., New furanoflavanoids, intestinal alpha-glucosidase inhibitory and free-radical (DPPH) scavenging, activity from antihyperglycemic root extract of *Derris indica* (Lam.), *Bioorg. Med. Chem. Lett.*, 2009; 17: 5170-5175.

35. Essa MM, Subramanian P, Suthakar G, et al., Protective influence of *Pongamia pinnata* (Karanja) on blood ammonia and urea levels in ammonium chloride-induced hyperammonemia, *J. Appl. Biomed.*, 2005; 3: 133-138.

36. Anuradha R, Krishnamoorthy P, Antioxidant activity of methanolic extract of *Pongamia pinnata* on lead acetate induced hepatic damage in rats, *Afr. J. Biochem. Res.*, 2011; 5: 348-351.

37. Vadivel V, Biesalski HK, Contribution of phenolic compounds to the antioxidant potential and type II diabetes related enzyme inhibition properties of *Pongamia pinnata* L. Pierre seeds, *Process. Biochem.*, 2011; 46: 1973-1980.

38. Bajpai VK, Rahman A, Shukla S, et al., Antibacterial activity of leaf extracts of *Pongamia pinnata* from India, *Pharm. Biol.*, 2009; 47: 1162-1167.

39. Elanchezhiyan M, Rajarajan S, Rajendran P, et al., Antiviral properties of the seed extract of an Indian medicinal plant, *Pongamia pinnata*, Linn., against herpes simplex viruses: *in-vitro* studies on vero cells, *J. Med. Microbiol.*, 1993; 38: 262-264.

40. Manigauha A, Patel S, Monga J, et al., Evaluation of anticonvulsant activity of *Pongamia pinnata* Linn in experimental animals, *Int. J. Pharm. Tech. Res.*, 2009; 4: 1119-1121.

41. Essa MM, Subramanian P, Protective role of pongamia pinnata leaf extract on tissue antioxidant status and lipid peroxidation in ammonium chloride-induced hyperammonemic rats., *Toxicol. Mech. Methods.*, 2006; 16: 477-483.

42. Nirmal SA, Malwadkar G, Laware RB, Anthelmintic activity of *Pongamia glabra*, *Songklanakarin. J. Sci. Technol.*, 2007; 29: 755-757.

43. Deshmukh P, Hooli AA, Holihosur SN, Screening of cold ethyl alcohol extract of *Pongamia pinnata* for insecticidal properties against *Spodoptera litura* Fabricius, *J. Oilseeds. Res.*, 2009; 26: 181-182.

44. George S, Bhalerao SV, Lidstone EA, et al., Cytotoxicity screening of Bangladeshi medicinal plant extracts on pancreatic cancer cells., *BMC Complement. Altern. Med.*, 2010; 10: 52-52.

45. Rao RR, Chaturvedi V, Babu KS, et al., Synthesis and anticancer effects of pongamol derivatives on mitogen signaling and cell cycle kinases, *Med. Chem. Res.*, 2012; 21: 634-641.

46. Tamrakar AK, Yadav PP, Tiwari P, et al., Identification of pongamol and karanjin as lead compounds with antihyperglycemic activity from *Pongamia pinnata* fruits, *J. Ethnopharmacol.*, 2008; 118: 435-439.

47. Wang W, Wang J, Li N, et al., Chemopreventive flavonoids from *Millettia pulchra* Kurz var-laxior (Dunn) Z.Wei (Yulangsan) function as Michael reaction acceptors, *Bioorg. Med. Chem. Lett.*, 2015; 25: 1078-1081.

48. Joshi P, Sonawane VR, Williams IS, et al., Identification of karanjin isolated from the Indian beech tree as a potent CYP1 enzyme inhibitor with cellular efficacy via screening of a natural product repository, *MedChemComm*, 2018; 9: 371–382.

49. Horley NJ, Beresford KJ, Chawla T, et al., Discovery and characterization of novel CYP1B1 inhibitors based on heterocyclic chalcones: Overcoming cisplatin resistance in CYP1B1-overexpressing lines, *Eur. J. Med. Chem.*, 2017; 129: 159-174.

50. Bharate SB, Sharma R, Joshi P, et al., Furanochalcones and furanoflavones as inhibitors of CYP1A1, CYP1A2 and CYP1B1 for cancer chemoprevention, *WO2018029710, February 15, 2018.*

51. Sharma R, Vishwakarma RA, Bharate SB, An efficient transformation of furanohydroxychalcones to furanoflavones via base mediated intramolecular tandem-o-arylation and C-O bond cleavage: a new approach for the synthesis of furanoflavones, *Org. Biomol. Chem.*, 2015; 13: 10461-10465.

52. Basu S, Shaik AN, Is there a paradigm shift in use of microsomes and hepatocytes in drug discovery and development?, *ADMET & DMPK*, 2016; 4: 114-116.

53. Rangaswami S, Seshadri TR, Chemistry of pongamol. Part I, *Proc. Indian Acad. Sci.*, 1942; 15: 417-423.

54. Parmar VS, Rathore JS, Jain R, et al., Occurrence of pongamol as the enol structure in *Tephrosia purpurea*, *Phytochemistry*, 1989; 28: 591-593.

55. Cui J, Meng Q, Zhang X, et al., Design and Synthesis of New alpha-Naphthoflavones as Cytochrome P450 (CYP) 1B1 Inhibitors To Overcome Docetaxel-Resistance Associated with CYP1B1 Overexpression, *Journal of medicinal chemistry*, 2015; 58: 3534-3547.

56. Peng CH, Huang CN, Wang CJ, The anti-tumor effect and mechanisms of action of penta-acetyl geniposide, *Curr. Cancer Drug Targets*, 2005; 5: 299-305.

57. Yang L, Liu H, Long M, et al., Peptide SA12 inhibits proliferation of breast cancer cell lines MCF-7 and MDA-MB-231 through G0/G1 phase cell cycle arrest, *Onco. Targets Ther.*, 2018; 11: 2409-2417.

58. Yoshida A, Lee EK, Diehl JA, Induction of therapeutic senescence in vemurafenib-resistant melanoma by extended inhibition of CDK4/6, *Cancer Res.*, 2016; 76: 2990-3002.

59. Murphy CG, Dickler MN, The role of CDK4/6 inhibition in breast cancer, *The oncologist*, 2015; 20: 483-490.

60. Sheppard KE, McArthur GA, The cell-cycle regulator CDK4: an emerging therapeutic target in melanoma, *Clin. Cancer Res.*, 2013; 19: 5320-5328.

61. Vismaya, Eipeson WS, Manjunatha JR, et al., Extraction and recovery of karanjin: A value addition to karanja (*Pongamia pinnata*) seed oil, *Ind. Crops Prod.* , 2010; 32: 118–122.

62. Gupta RK, Krishnamurti M, New dibenzoylmethane and chalcone derivatives from *Milletia ovalifolia* seeds, *Phytochemistry*, 1977; 16: 1104-1105.

63. Edayadulla N, Ramesh P, A new prenylated acetophenone from the root bark of *Derris indica*, *Nat. Prod. Commun.*, 2012; 7: 1325-1326.

64. Na Z, Song QS, Hu HB, Flavonoids from twigs of *Millettia pubinervis*, *Nat. Prod. Commun.*, 2014; 9: 1721-1722.

65. Mahale S, Bharate SB, Manda S, et al., Biphenyl-4-carboxylic acid [2-(1H-indol-3-yl)-ethyl]-methylamide (CA224), a nonplanar analogue of fascaplysin, inhibits Cdk4 and tubulin polymerization: evaluation of in vitro and in vivo anticancer activity, *J. Med. Chem.*, 2014; 57: 9658-9672.

66. Serrano M, Lin AW, McCurrach ME, et al., Oncogenic ras provokes premature cell senescence associated with accumulation of p53 and p16INK4a, *Cell*, 1997; 88: 593-602.

67. Georgakopoulou EA, Tsimaratou K, Evangelou K, et al., Specific lipofuscin staining as a novel biomarker to detect replicative and stress-induced senescence. A method applicable in cryo-preserved and archival tissues, *Aging*, 2013; 5: 37-50.

Graphical Abstract